Chapter 2

Tropical Cyclone Center Determination Algorithm by Texture and Gradient of Infrared Satellite Image

Chang-Jiang Zhang, Qi Luo, Yuan Chen, Juan Lu,
Li-Cheng Xue and Xiao-Qin Lu

Additional information is available at the end of the chapter

http://dx.doi.org/10.5772/intechopen.79831

Abstract

A novel algorithm for tropical cyclone (TC) center determination is presented by using texture and gradient of infrared satellite image from geostationary satellite. Except those latter disappearing TC satellite images that are little valuable to a TC center determination, generally other periods of TC, all have an inner core. And the centers are generally determined in the inner core. Based on this, an efficient TC center determination algorithm is designed. First, the inner core of a TC is obtained. Then, according to the texture and gradient information of the inner core, the center location of the TC is determined. The effectiveness of the proposed TC center determination algorithm is verified by using Chinese FY-2C stationary infrared satellite image. And the location result is compared with that of the "tropical cyclone yearbook," which was compiled by Shanghai Typhoon Institute of China Meteorological Administration. Experimental results show that the proposed algorithm can provide a new technique that can automatically determine the center location for a TC based on infrared satellite image.

Keywords: tropical cyclone, infrared satellite image, center location, gradient, texture

1. Introduction

Tropical cyclone (TC) is one of the most serious natural disasters in the world. Satellite remote sensing technology can not only observe the whole situation but also the structural characteristics and center information of a TC. It is the current main method of the TC center location.

Dvorak technique (DT) is widely used to TC center location. DT, which was proposed by [1, 2] in the 1970s was the most important method for TC analysis in the world. Nowadays, based

on the DT, advanced Dvorak technologies [3–5] were developed to determine the TC center location. Li et al. [6] put forward a new artificial intelligence algorithm for the eye TC center location. First, the image segmentation technique was used to extract the TC cloud features. And then, the mathematic morphology opening operation and the filling operation are used to obtain the contour of the TC eye. The gravity calculation method is applied to locate the TC center. Comparing the data to the Central Meteorological Observatory of China, the experimental results show that the deviation is smaller. Li et al. [7] proposed an improved genetic algorithm to determine the TC center location. The theoretical analysis and experimental results show that this method is reasonable and effective. Yang et al. [8] combined pattern matching with the vector field analysis to determine the TC center position. The proposed method is very efficient for the TCs, which have clear spiral structure. Fan et al. [9] used 85 GHz vertical polarization channels in specail sensor microwave/imager (SSM/I) for TC center location. According to the distributed characteristics of brightness and temperature, the TC of its band is analyzed and classified. The average gap of the best route in the test results of TC is smaller. Wei et al. [10] presented a novel spiral band model to automatically locate the TC center. And particle swarm optimization was used to optimize the model parameters. Experimental results show that this model can achieve the best average error in both latitude and longitude in comparison with the best track data. Zhang et al. [11] proposed a novel intelligent automatic system framework, which was based on the image process technology to locate the TC center. According to the symmetry shape and spiral movement feature of TC, a rotation matching methodology is used to catch the track of TC. Compared with the data of Shanghai Meteorology Center, experimental results show that this system is efficient and the performance errors are acceptable for practical applications. Zheng et al. [12] established the TC forecast service production system based on geographic information system (GIS) technology and realized the function construction. It had met the requirements of the TC center forecast service production in the Central Meteorological Observatory. Recently, some researchers used deviation angle variance [13] and pattern matching algorithm [14] for TC center detection.

Although there are some advantages in the above methods, some defects are existing. The subjectivity of DT is stronger, and the degree of automation is limited. The location effect for the smaller intensity cyclone is poorer. The method based on mathematical morphology is suitable for tropical cyclone whose morphology characteristic can be identified easily. If it is applied to the weak or atypical morphology cyclone, a big deviation will be resulted. Intelligent learning method requires a lot of experimental data and experience accumulation. It is suitable for recognizing the particular structures. Wind field analysis method is applicable to locate the tropical cyclone center, which is weak and whose circulation center is not clear. When the intensity level of tropical cyclone is higher, the center location is not accurate because it is easily affected by the resolution and heavy rain [11]. The temperature/humidity structure retrieval method is also only applied to locate the tropical cyclone center whose intensity is strong. The tempo-spatial movement matching method applied movement information of adjacent satellite images to determine the TC center position [11]. But the computation burden of the method is large. Generally, center location for eye TCs has good results. But it is not very satisfying for non-eye TCs due to some reasons. Therefore, it is very important to improve the accuracy of automatic TC center location.

Here, we extract the inner core region from an infrared satellite image, which contains a TC initially. Then, according to the characteristic of the position of TC center, which is the intersection of the ambient airflow and the different textures between the inner core region and other cloud area, we determine the TC center further. And the texture is uniform and smooth in the inner core region. The gray values of the inner core region are higher than those which are on the edge of the TC. So, we calculate the fractal dimension and 3-s order statistical parameters of a gray-gradient co-occurrence matrix to determine the inner core region of the TC. Then, according to the gradient information of the inner core region, the center location of the TC is determined.

2. Extract the inner core region

In general, the TC cloud consists of spiral cloud band, inner core region, and TC center area. If the inner core region is extracted from the TC cloud, it will reduce the area, which contains the TC center. The average gray values of the inner core region in an infrared satellite image are high and the difference between the gray values of pixels is small. The gray-gradient co-occurrence matrix (GGCOM) can be used to measure the gray value difference in an infrared satellite image. The fractal dimension is a useful to represent texture characteristics of the infrared satellite image. The inner core region of a TC is extracted by combining the fractal dimension with GGCOM.

2.1. GGCOM

The analysis method of the gray-gradient co-occurrence matrix is to extract the texture feature by the comprehensive information about the gray values and gradient of the images. Because the scales of different characteristic parameters are different, we normalize the gray values and gradient values of the image. Details for GGCOM computation refer to our previous work [15].

2.2. Fractal dimension

According to the characteristics of the satellite cloud image, we use the method by Sarkar and Chaudhuri [16] to calculate the box fractal dimension.

If the size of image is $N \times N$, we shrink the image into an value S_n by the plotting scale, $1 < S_n \le N/2$, and S_n $(1 \le n \le N)$ is an integer. So, we have an estimate of the scale r, which is $r = N/S_n$.

Let an image be considered as a three-dimensional space (x, y, z). Here, (x, y) means two-dimensional coordinate, and z means the gray value of the image element. So, (x, y) plane is divided into $S_n \times S_n$ grid. There is a series of boxes, whose bottom is $S_n \times S_n$ in each grid. The height h of box can be calculated by the gray level L of the whole image, namely $[L/h] = [N/S_n]$. Each box is labeled from down to up as $1, 2, 3, \cdots$, and in which box the maximum and minimum image gray values of the (m, n) grid $(1 \le m \le N)$ fall is checked. If the maximum value falls into a and the minimum value falls into b, then $n_r = a - b + 1$. N_r, which is the number of the boxes that cover the entire image can be described as:

$$N_r = \sum_{m,n} n_r(m, n) \tag{1}$$

In this way, N_r is calculated by each r. r changes as the change of s. The minimum linear fit is used for $\log(N_r)$ and $\log(1/r)$, and then the slope is calculated, namely Q, which is the fractal dimension.

$$Q = \log N_r / \log(1/r) \tag{2}$$

It is necessary to consider how to select the window of subimage and r calculates the scale of fractal dimension. The window size of subimage is too small to lose the important texture or is too large to mix the edge pixels with other pixels of the image area. It affects the selection of the texture feature. Choosing different scales will also affect the correctness of the linear fitting,that is, it affects the fractal dimension Q.

2.3. Extraction of inner core region

Through a large number of experimental satellite cloud images, we select the parameters, which can reflect the characteristic of TC cloud image clearly. The specific standard for choosing is as follows: the difference of this characteristic in different TC cloud images, inner core region, and other cloud regions is the biggest. And this characteristic is not sensitive for the inner core region or other cloud region, that is, it is consistent between different samples. In this chapter, average gray scale, small gradient advantage, and gradient uniformity of the GGCOM are used as features to locate the center of the TC [15]. Then, the inner core region of TC is determined by combining GGCOM with fractal dimension.

The scales of the above four characteristic parameters vary widely because the physical significance and scope of the different characteristic parameters are different. We test 10 groups of the main cloud region of the satellite cloud images whose size is 512 × 512: (1) infrared channel 1 cloud image of the No. 0513 TC "Talim," which was obtained at 0 o'clock on August 29, 2005 (20050829_0000_IR1); (2) infrared channel 2 cloud image of the No. 0513 TC "Talim," which was obtained at 6 o'clock on August 29, 2005 (20050829_0600_IR2); (3) infrared channel 1 cloud image of the No. 0513 TC "Talim," which was obtained at 21 o'clock on August 29, 2005 (20050829_2100_IR1); (4) infrared channel 2 cloud image of the No. 0513 TC "Talim," which was obtained at 18 o'clock on August 30, 2005 (20050830_1800_IR2); (5) infrared channel 1 cloud image of the No. 0713 TC "Wipha," which was obtained at 0 o'clock on September 16, 2007 (20070916_0000_IR1); (6) infrared channel 2 cloud image of the No. 0713 TC "Wipha," which was obtained at 18 o'clock on September 16, 2007 (20070916_1800_IR2); (7) infrared channel 1 cloud image of the No. 0814 TC "Hagumi," which was obtained at 12 o'clock on September 22, 2008 (20080922_1200_IR1); (8) infrared channel 2 cloud image of the No. 0814 TC "Hagumi," which was obtained at 0 o'clock on September 24, 2008 (20080924_0000_IR2); (9) infrared channel 1 cloud image of the No. 0601 TC "Chanchu," which was obtained at 6 o'clock on May 11, 2006 (20060511_0600_IR1); and (10) infrared channel 2 cloud image of the No. 0601 TC "Chanchu," which was obtained at 12 o'clock on May 12, 2006 (20060512_1200_IR2). All the time are the universal time. About 10 groups of the satellite cloud images are

shown in **Figure 1**. The corresponding main bodies of the satellite cloud images are shown in **Figure 2**. Here, the fractal dimension Q, the average gray scale $\bar{G}$, the small gradient $\bar{S}$, and the inhomogeneity of the gradient distribution $\bar{D}$ are the characteristics of the main cloud of images. The four characteristics parameter values of these 10 test cloud images are shown in **Table 1**.

From **Table 1**, we can see that the range of the fractal dimension Q is from 1 to 3; the range of $\bar{S}$ is from 0 to 1; the range of $\bar{D}$ is on the amount of 10^5; and the range of $\bar{G}$ is from 0 to 200. The difference between small and big components is large. The small component is easy to be ignored when the Euclidean distance is measured. The aforementioned four parameters should be normalized so that the same weight is used to compute the Euclidean distance.

The steps of determining the inner core region are as follows:

Step 1. Separate main body of the TC from an infrared satellite image based on our previous work [17];

Step 2. Because the size of the selection of the test cloud images is 512 × 512 or 256 × 256, we use 39 × 39 window, which is determined by the experiments to compute fractal dimension and GGCOM;

Step 3. Normalize four parameters to compute the difference value ΔD_w ($w = 1, 2, \cdots, 39$) of the fractal dimension and GGCOM;

Step 4. Get the values of ΔD_w in each window;

Step 5. Compare with each ΔD_w, the window, which ΔD_w is the biggest is determined as the inner core region of TC.

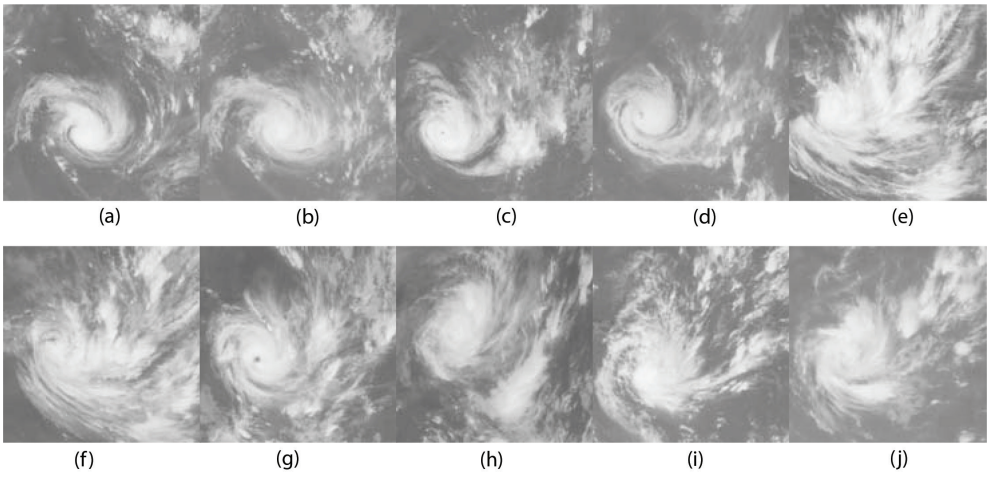

Figure 1. Ten groups of infrared channel satellite cloud images. (a) 20050829_0000_IR1; (b) 20050829_0600_IR2; (c) 20050829_2100_IR1; (d) 20070916_0000_IR1; (e) 20070916_0000_IR1; (f) 20070916_1800_IR2; (g) 20080922_1200_IR1; (h) 20080924_0000_IR2; (i) 20060511_0600_IR1; (j) 20060512_1200_IR2.

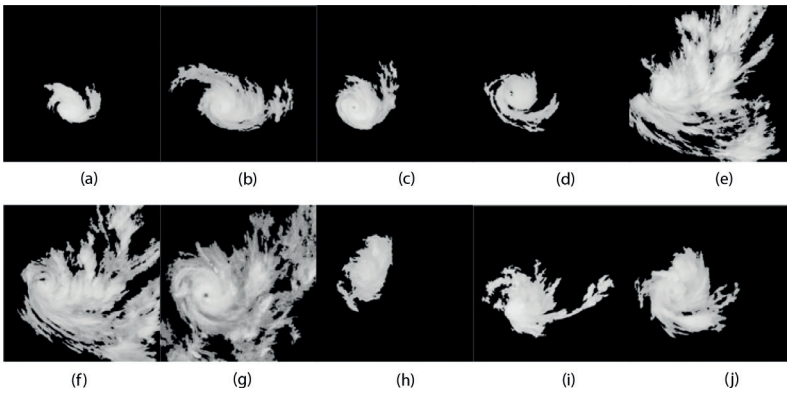

Figure 2. Corresponding main cloud of satellite cloud image. (a) 20050829_0000_IR1; (b) 20050829_0600_IR2; (c) 20050829_2100_IR1; (d) 20070916_0000_IR1; (e) 20070916_0000_IR1; (f) 20070916_1800_IR2; (g) 20080922_1200_IR1; (h) 20080924_0000_IR2; (i) 20060511_0600_IR1; (j) 20060512_1200_IR2.

Satellite cloud image	Q	$\bar{S}$	$\bar{D}$	$\bar{G}$
20050829_0000_IR1	1.2954	0.9706	2.4513×10^5	12.2469
20050829_0600_IR2	1.2189	0.9039	2.1138×10^5	31.9240
20050829_2100_IR1	1.2089	0.9414	2.3005×10^5	20.5072
20050830_1800_IR2	1.2806	0.9522	2.3546×10^5	18.2701
20070916_0000_IR1	1.1528	0.6705	1.1624×10^5	110.3207
20070916_1800_IR2	1.1633	0.6720	1.1686×10^5	100.5608
20080922_1200_IR1	1.1642	0.6264	1.0208×10^5	100.7266
20080924_0000_IR2	1.2041	0.9532	2.3573×10^5	19.4768
20060511_0600_IR1	1.1911	0.9210	2.1964×10^5	31.7581
20060512_1200_IR2	1.1729	0.8973	2.0791×10^5	40.3393

Table 1. Characteristic parameters of the main cloud in 10 groups of satellite cloud images.

Extracting the inner core region not only can reduce the region of TC center but also can eliminate the influence of the outer spirals. It can make the foundation for extracting the small gradient information. Based on these two purposes, it is not important whether to completely extract the inner core region. The key is to extract the main part of the inner core region. So a rough estimation by the size of TC cloud is feasible. The experiments also prove that the size of window can satisfy the need as per the above algorithm.

3. Determine the center of TC

It is assumed that whatever the type of the bending cloud, strong wind, eye cloud region, or type of center closed clod cloud region, the center of TC is almost located in the inner core

region. After extracting the inner core region, we can determine the center of TC by the inner core region. The region near TC center has obviously the warm structure. The infrared brightness temperature gradient of the inner core region is small compared with the TC eye. The richest gradient region can be considered as the TC center region.

3.1. Compute the gradient information of inner core region

Before computing the gradient of the inner core region, Gaussian filter reduces the noise of the main body of the TC. The image and Gaussian smoothing filter are convolved as follows:

$$J(i,j) = S(i,j;\sigma^2) * I(i,j) \tag{3}$$

where $S(i,j;\sigma^2)$ represents the Gaussian function and σ^2 indicates variance. How to choose proper σ^2 is very important. $I(i,j)$ shows TC main body image.

Different variance σ^2 will be used to extract different gradient information from the main body cloud of a TC. The infrared channel 2 cloud image of the No. 0601 TC "Chanchu," which was obtained at 12 o'clock on May 12, 2006 (20060512_1200_IR2) is an example (see in **Figure 3(a)**). The image in which the variance is chosen as $\sigma^2 = 0.5$ is shown in **Figure 3(b)**. The image in which the variance is chosen as $\sigma^2 = 1.0$ is shown in **Figure 3(c)**. The image in which the variance is chosen as $\sigma^2 = 1.5$ is shown in **Figure 3(d)**. The image in which the variance is chosen as $\sigma^2 = 2.0$ is shown in **Figure 3(e)**. The image in which the variance is chosen as $\sigma^2 = 2.5$ is shown in **Figure 3(f)**.

From **Figure 3**, we can see that the influence of σ^2 for extracting the gradient information is big. When the value of σ^2 is small, the accuracy of the edge position is high. But edge details change a lot. When the value of σ^2 is small, the effect of the smooth is large and the details lose a lot.

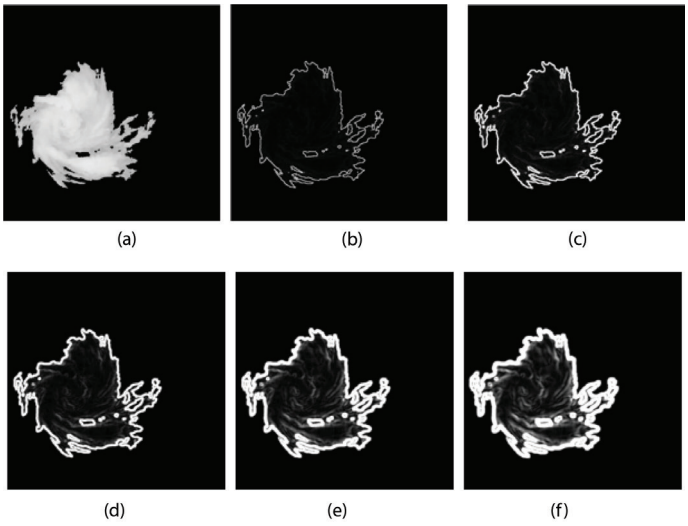

Figure 3. The influence of σ^2 for extracting the gradient information. (a) Main body cloud of TC; (b) $\sigma^2 = 0.5$; (c) $\sigma^2 = 1.0$; (d) $\sigma^2 = 1.5$; (e) $\sigma^2 = 2.0$; (f) $\sigma^2 = 2.5$.

Figure 4. The gradient information and texture of the inner core region. (a) Gradient information when σ^2 =2.0; (b) gradient information after enhancing and (c) edge detection by Canny.

The accuracy of the edge position is low. And the gradient information is rich. Based on it, we choose the variance σ^2 is 2.0. For this condition, the gradient image of the inner core is obvious.

In order to further enhance the gradient in the inner core region. A constant 5 is multiplied to the gradient image. Canny operator is used to determine the concentrated gradient region. This region should contain the TC center. The effect of the gradient information extracted from the inner core region is shown in **Figure 4**. **Figure 4(a)** is the gradient information of the inner core region when σ^2 = 2.0. **Figure 4(b)** is the gradient information of the enhanced image. **Figure 4(c)** is the result of the edge detection by Canny operator.

We can see from **Figure 4(a)** that the gradient information of the image is not obvious. In **Figure 4(b)**, the gradient information after enhancing the image is clearer. It is convenient to do the edge detection by the Canny operator. The gradient and texture information of the inner core region is very obvious in **Figure 4(c)**.

3.2. Determine the center of TC

The region whose gradient information is the most abundant in the inner core region is the region which contains the TC center. The gradient information, which is extracted from the clear eye TC is the obvious characteristic. According to edge information of the image in Section 3.1, which is the gradient information and expresses the texture feature of the image, the region whose texture is the most abundant in the inner core region, which is called the region of interest (ROI), is the region, which contains the TC center. The geometric center of the ROI is defined as the TC center.

Generally, the average diameter for a TC eye is 45 km or so. The spatial resolution for FY-2C satellite image is 5 km. Therefore, a 9 × 9 mask is used to search the inner core region. If a closed curve is found in the inner core region, the centroid of the curve is determined as TC center. Otherwise, the region whose intersection lines are the most is chosen as the ROI.

4. Results and discussion

Infrared satellite images from Chinese geostationary satellite FY-2C are used to verify the performance of the proposed algorithm in this paper. The TC center location is used to test the

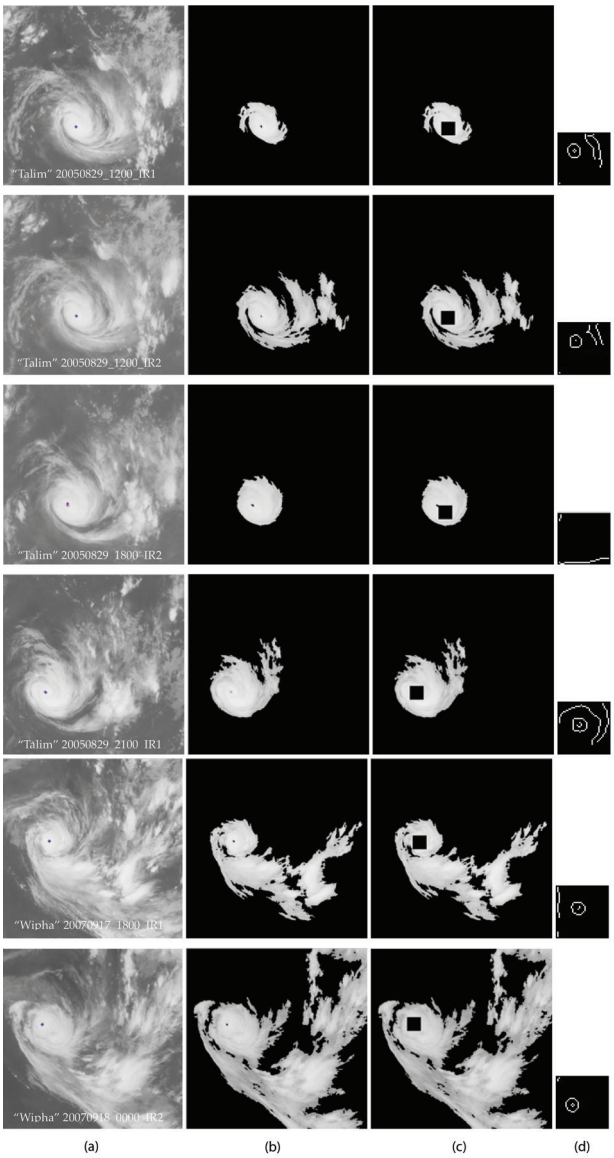

Figure 5. TC center location of eye TCs satellite images. (a) Result of the TC center location; (b) main cloud of TC; (c) position of the inner core region and (d) texture.

infrared channel 1 and the infrared channel 2 satellite images, respectively. Six groups of eye TC and six groups of non-eye TC, which are the satellite images are used to verify the proposed algorithm. All the satellite images are 512 × 512. The test satellite images of the eye TC include: (1) infrared channel 1 satellite image of the No. 0513 TC "Talim," which was obtained at 12 o'clock on August 29, 2005 (20050829_1200_IR1); (2) infrared channel 2 satellite image of the

No. 0513 TC "Talim," which was obtained at 12 o'clock on August 29, 2005 (20050829_1200_IR2); (3) infrared channel 2 satellite image of the No. 0513 TC "Talim," which was obtained at 18 o'clock on August 29, 2005 (20050829_1800_IR2); (4) infrared channel 1 satellite image of the No. 0513 TC "Talim," which was obtained at 21 o'clock on August 29, 2005 (20050829_2100_IR1); (5) infrared channel 1 satellite image of the No. 0713 TC "Wipha," which was obtained at 18 o'clock on September 17, 2007 (20070917_1800_IR1); and (6) infrared channel 2 satellite image of the No. 0713 TC "Wipha," which was obtained at 0 o'clock on September 18, 2007 (20070918_0000_IR2). The test satellite images of the non-eye TC include: (1) infrared channel 1 satellite image of the No. 0513 TC "Talim," which was obtained at 18 o'clock on August 27, 2005 (20050827_1800_IR1); (2) infrared channel 1 satellite image of the No. 0513 TC "Talim," which was obtained at 0 o'clock on August 29, 2005 (20050829_0000_IR1); (3) infrared channel 1 satellite image of the No. 0513 TC "Talim," which was obtained at 12 o'clock on August 28, 2005 (20050828_1200_IR1); (4) infrared channel 2 satellite image of the No. 0513 TC "Talim," which was obtained at 12 o'clock on August 28, 2005 (20050828_1200_IR2); (5) infrared channel 1 satellite image of the No. 0713 TC "Wipha," which was obtained at 0 o'clock on September 17, 2007 (20070917_0000_IR1); and (6) infrared channel 2 satellite image of the No. 0713 TC "Wipha," which was obtained at 0 o'clock on September 17, 2007 (20070917_ 0000_IR2). The time of these experimental images is the universal time.

4.1. Experimental group of eye TC center location

Figure 5(a)–(d) represents six eye TC satellite images and their center location results. TC center position from China Meteorological Administration is used as the reference center position. In this paper, blue "*" symbol and red "+" symbol, respectively, indicate the center position by the proposed method and reference center position.

We can see from above figures that the location results by the proposed TC center location algorithm are very close to the reference positions. Namely, the results are very close to the real center of TC. After the extraction of the main body cloud of a TC, the selected inner core region almost contains the cloud area of the eye of TC. And the texture of the inner core region is clear. The distance of the center location by the proposed algorithm and the reference position is so little. So it is difficult to identify the difference between them by the naked eye. Since

TC cloud image	Result of center location		Reference values		Error (km)
	North latitude (°)	East longitude (°)	North latitude (°)	East longitude (°)	
20050829_1200_IR1	20.95	131.89	21.00	131.90	5.66
20050829_1200_IR2	20.95	131.89	21.00	131.90	5.66
20050829_1800_IR2	21.15	130.43	21.20	130.70	30.48
20050829_2100_IR1	21.19	130.21	21.30	130.10	17.27
20070917_1800_IR1	23.93	124.67	23.90	124.60	8.45
20070918_0000_IR2	24.43	123.71	24.40	123.60	12.66

Table 2. The center location errors of the experimental eye TC group.

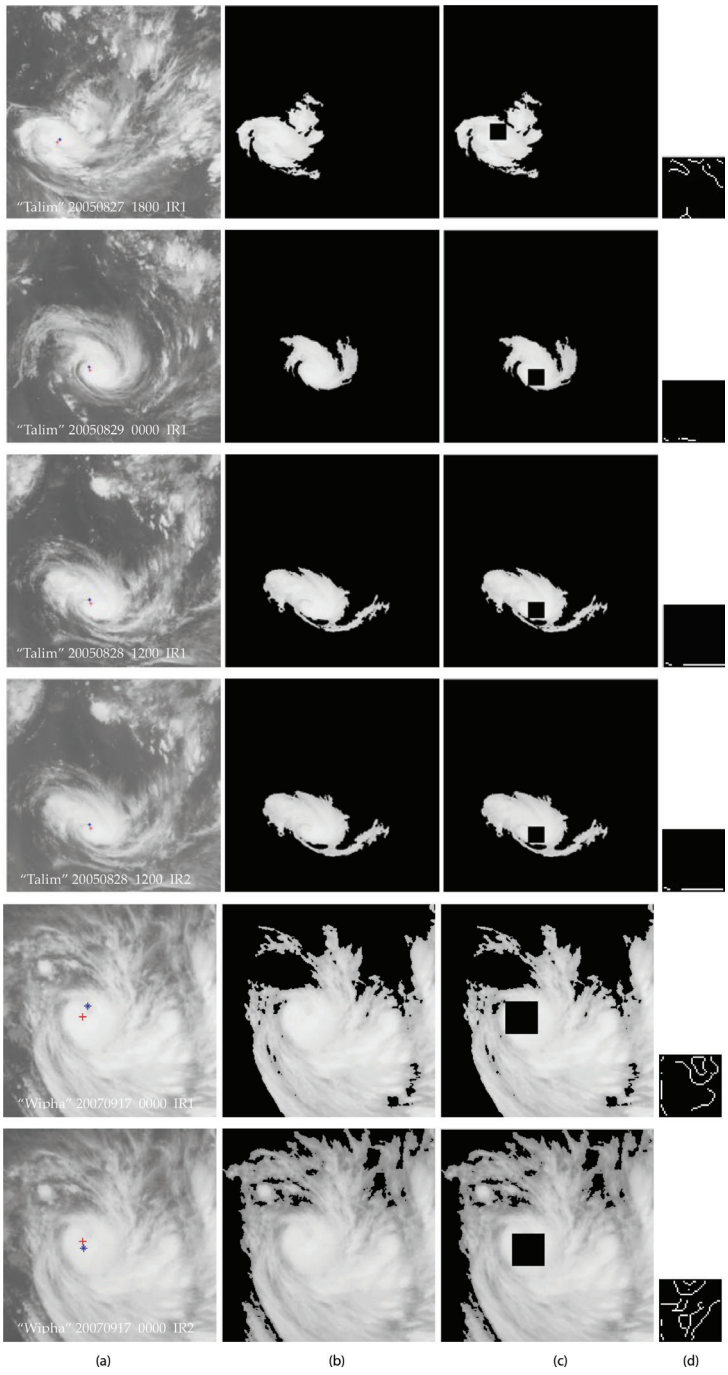

Figure 6. TC center location of non-eye TCs. (a) Result of the TC center location; (b) main cloud of TC; (c) position of the inner core region and (d) texture.

TC cloud image	Result of center location		Reference values		Error (km)
	North latitude (°)	East longitude (°)	North latitude (°)	East longitude (°)	
20050827_1800_IR1	17.59	139.43	17.90	139.90	62.50
20050829_0000_IR1	20.49	133.85	20.40	134.30	50.94
20050828_1200_IR1	20.01	136.17	19.90	136.70	60.08
20050828_1200_IR2	20.01	136.17	19.90	136.70	60.08
20070917_0000_IR1	22.07	126.91	22.40	127.70	95.03
20070917_0000_IR2	22.37	128.13	22.40	127.70	47.85

Table 3. The center location errors of the experimental non-eye TC group.

the length of 1° latitude is about 111 km and the length of 1° longitude is about 111 km all over the world, we calculate the distance error of the TC center position by the longitude and latitude errors. The center position errors of the six groups of eye TC are shown in **Table 2**.

In **Table 2**, we can find that the error of the TC center location by the proposed algorithm is below 40 km. And it is suitable for the infrared channel 1 and the infrared channel 2 cloud images.

4.2. Experimental group of non-eye TC center location

Figure 6(a)–(d) represent six non-eye TC satellite images and their center location results.

We can see from the figures that the located results by the proposed TC center location algorithm are very close to the reference positions. The effect of the non-eye TC center location is good. In order to get the more accurate location error, we calculate the distance error of the TC center position by the longitude and latitude errors. The center position errors of the six experimental groups of the non-eye TC center location are shown in **Table 3**.

In **Table 3**, we can find that the error of five groups of the non-eye TC center location by the proposed algorithm is below 70 km. Only the error of one group is more than 70 km, but it is below 100 km. In all, the proposed algorithm is suitable to be used to determine the center position for a TC by using the infrared channel 1 and the infrared channel 2 cloud images. Although the accuracy of the non-eye TC center location is slightly less than that of the eye TC center location, the error is small for the non-eye TC in which the texture is not prominent.

5. Conclusions

An effective TC center location algorithm, which is based on the fractal feature features and gradient of the infrared satellite cloud images, is proposed. The proposed algorithm is based on the assumption that the centers of a TC, which belongs to different development stages are mostly located in the inner core region. The inner core region is determined firstly. Then

special gradient information and texture of the TC center are used to determine the center of TC. The proposed algorithm can be applied in the eye TC center location and the non-eye TC center location. The accuracy of the location by this proposed algorithm is higher. Moreover, the calculation of the proposed algorithm is simpler than that of the existing TC center location methods, such as the wind field analysis method, intelligent learning method based on the spiral fitting, tempo-spatial movement matching method, and so on. The proposed method is not proper to disorganized or weak TCs. Further work is needed to improve the location accuracy of TCs by using new features or techniques.

Acknowledgements

The part of work in this paper is supported by Natural Science Foundation of China (No. 41575046, No. 40805048, and No. 11026226), Project of Commonweal Technique and Application Research of Zhejiang Province of China (No. 2016C33010, No. 2012C23027), and Natural Science Foundation of Zhejiang Province of China (No. LY13D050001).

Author details

Chang-Jiang Zhang[1]*, Qi Luo[1], Yuan Chen[1], Juan Lu[1], Li-Cheng Xue[1] and Xiao-Qin Lu[2]

*Address all correspondence to: zcj74922@zjnu.edu.cn

1 Department of Electronic and Communication Engineering, College of Mathematics, Physics and Information Engineering, Zhejiang Normal University, Jinhua, China

2 Shanghai Typhoon Institute of China Meteorological Administration, Shanghai, China

References

[1] Dvorak VF. Tropical cyclone intensity analysis and forecasting from forecasting from satellite imagery. Monthly Weather Review. 1975;**103**(5):420-430. DOI: 10.1175/1520-0493(1975)103%3C0420:TCIAAF%3E2.0.CO;2

[2] Yang Hq, Yang Ym. Progress in objective position methods of tropical cyclone center using satellite remote sensing. Journal of Tropical Oceanography. 2012;**31**(2):15-27

[3] Knaff JA, Brown DP, Courtney J, Gallina GM, Beven JL. An evaluation of Dvorak technique-based tropical cyclone intensity estimates. Weather and Forecasting. 2010; **25**(5):1362-1379. DOI: 10.1175/2010WAF2222375.1

[4] Olander TL, Velden CS. The advanced Dvorak technique: continued development of an objective scheme to estimate tropical cyclone intensity using geostationary infrared satellite imagery. Weather and Forecasting. 2007;**22**(2):287-298. DOI: 10.1175/WAF975.1

[5] Velden C, Harper B, Wells F, Beven JL, Zehr R, Olander T, Mayfield M, Guard CC, Lander M, Edson R, et al. The Dvorak tropical cyclone intensity estimation technique: A satellite-based method that has endured for over 30 years. Bulletin of the American Meteorological Society. 2006;**87**(9):1195-1210. DOI: 10.1175/BAMS-87-9-1195

[6] Li H, Huang XY, Qin DY. Research the artificial intelligent algorithm for positioning of eyed typhoon with high resolution satellite image. In: Proceedings of the 2012 5th International Joint Conference on Computational Sciences and Optimization; 23-26 June 2012; Harbin. Heilongjiang: IEEE; 2012. pp. 889-891

[7] Li Y, Chen X, Fei SM, Mao KF, Zhou K. The study of a linear optimal location the typhoon center automatic from IR satellite cloud image. In: Proceedings of SPIE—The International Society for Optical Engineering; 24-24 May 2011; Beijing: SPIE; 2011. p. 81932F

[8] Yang J, Wang H. Positioning tropical cyclone center in a single satellite image using vector field analysis. Lecture Notes in Electrical Engineering. 2013;**256**:37-44. DOI: 10.1007/978-3-642-38466-0_5

[9] Fan Z. Application of satellite SSM/I data in the typhoon center location and maximum wind speed estimation [D]. Taoyuan: National Central University in Taiwan; 2004. pp. 1-2

[10] Wei K, Jing ZL, Li YX, Liu SL. Spiral band model for locating tropical cyclone centers. Pattern Recognition Letters. 2011;**32**(6):761-770. DOI: 10.1016/j.patrec. 2010. 12.011

[11] Zhang QP, Lai LL, Sun WC. Intelligent location of tropical cyclone center. In: 2005 International Conference on Machine Learning and Cybernetics, ICMLC 2005; 2005; pp. 423-428

[12] Zheng W, Wu H, Luo B, Liu Z, Lv Z, Sun L. Application of GIS to tropical cyclone product generation system. Journal of Applied Meteorological Science. 2010;**21**(2):250-256

[13] Piñeros MF, Ritchie EA, Scott Tyo J. Objective measures of tropical cyclone structure and intensity change from remotely sensed infrared image data. IEEE Transactions on Geoscience and Remote Sensing. 2008;**46**(11):3574-3580. DOI: 10.1109/TGRS.2008.2000819

[14] Jin S, Wang S, Li X, Jiao L, Zhang JA, Shen D. A salient region detection and pattern matching-based algorithm for center detection of a partially covered tropical cyclone in a SAR image. IEEE Transactions on Geoscience and Remote Sensing. 2017;**55**(1):280-291. DOI: 10.1109/TGRS.2016.2605766

[15] Changjiang Z, Yuan C, Juan L. Typhoon center location algorithm based on fractal feature and gradient of infrared satellite cloud image. In: Proceedings of SPIE-International Symposium on Optoelectronic Technology and Application; 13-15 May, 2014; Beijing. p. 92990F

[16] Chaudhuri BB, Sarkar N. Texture segmentation using fractal dimension. IEEE Transactions on Pattern Analysis and Machine Intelligence. 1995;**17**(1):72-77. DOI: 10.1109/34.368149

[17] Mengyin F, Changjiang Z, Mei J. Wavelet transform approach to segment thermal image. Journal of Beijing Institute of Technology. 2003;**12**(suppl):33-38